Longitudinal Finger Rotation
Problems and Effects in Finger-Vein Recognition

Bernhard Prommegger, Christof Kauba and Andreas Uhl

Department of Computer Sciences
University of Salzburg

October 17, 2019

Overview

Outline

- The networks of blood vessel under the skin of the finger are unique
- Therefore, finger-vein characteristics are suitable for biometric applications
- Similar to fingerprints also images of the blood vessels can be used for authentication

Biometric finger vein recognition system

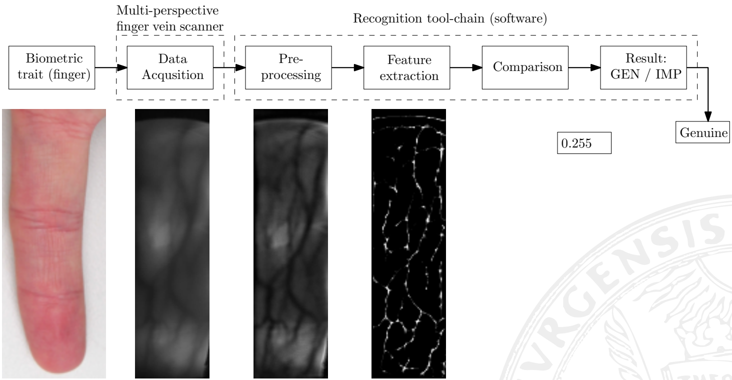

Figure: Basic components of a biometric recognition system

Finger-Vein Biometrics III

Recognition performance strongly depends on quality of acquired images.

Acquisition effected by internal

- NIR light source
- camera module
- sensor configuration
- ...

and external factors

- environmental conditions (temperature, humidity, ...)
- finger misplacements (including longitudinal finger rotation)
- ...

Advantages

- Resistant to forgery as vein structures are inside the finger and only visible in infrared light
- Liveness detection is possible
- No abrasion as with fingerprints
- Insensitive to finger surface conditions

Disadvantages

- Comparatively large capturing device
- Images have in general lower contrast and lower quality than fingerprint images
- Vein structures are influenced by temperature and physical activity
- Vein structure may be influenced by certain diseases or injuries

Outline

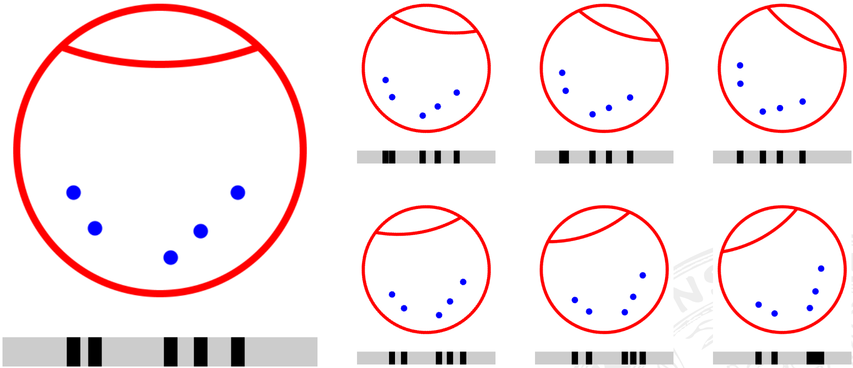

Figure: Finger longitudinal axis rotation principle: a schematic finger cross section showing five veins (blue dots) rotated from -10° to -30° (top row) and 10° to 30° (bottom row) in 10° steps. The projection of the vein pattern is different according to the rotation angle following a non-linear transformation.

The Problem of Longitudinal Finger Rotation II

Figure: Finger rotation example using an off-the-shelf commercial scanner

Outline

PLUSVein-Finger Rotation Data Set I

- Up to now only palmar (and one dorsal) data sets
- Evaluation of longitudinal finger rotation not possible
- New finger-vein data set providing images all around the finger (360°-view)
- Acquired using our custom build sensor

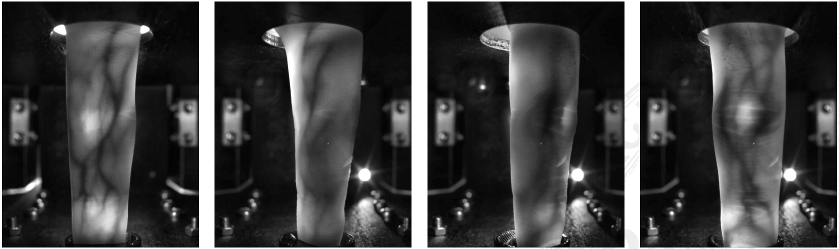

0° 60° 120° 180°

Figure: Example images of the data set acquired from 0° to 180° in 60° steps

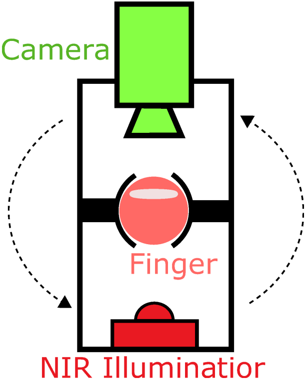

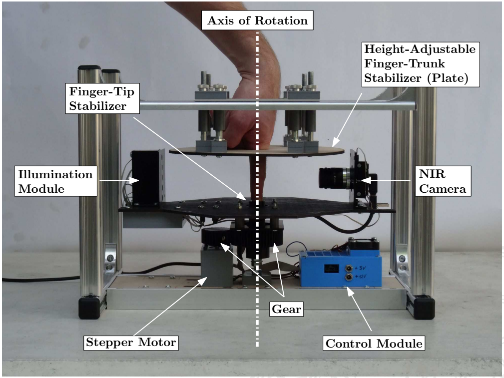

Figure: Left: Principle of the multi-perspective finger vein scanner, right: the scanner itself (originally published in [1], © 2018 IEEE)

Statistical data

- 63 subjects (27 female, 36 men)
- 11 nations (Austria, Brazil, China, Ethiopia, Germany, Hungary, Iran, Italy, Russia, Slovenia, USA), but mainly white Europeans (73%)
- Age: 18 (limited by national law) to 79 years
- Further acquisitions planed (33 additional subjects for PROTECT Multimodal DB [2], another session at PLUS planned)
- Containing the same subjects as the PLUSVein-FV3 Data Set [3], a data set that provides palmar and dorsal finger vein images acquired using two different sensors (laser/LED transillumination $\rightarrow$ poster session).

PLUSVein-Finger Rotation Data Set IV

Total data set

- 252 unique fingers (63 different subjects, 4 fingers per subject)
- 5 samples per finger
- 1.260 images per view
- Step-size: 1°
- 361 different views (0° + 360°)
- 454.860 images in total.

Used sub-set for this paper

- Range of ±90° around palmar view (0°)
- Step-size: 1°
- 181 different views
- 228.060 images in total.

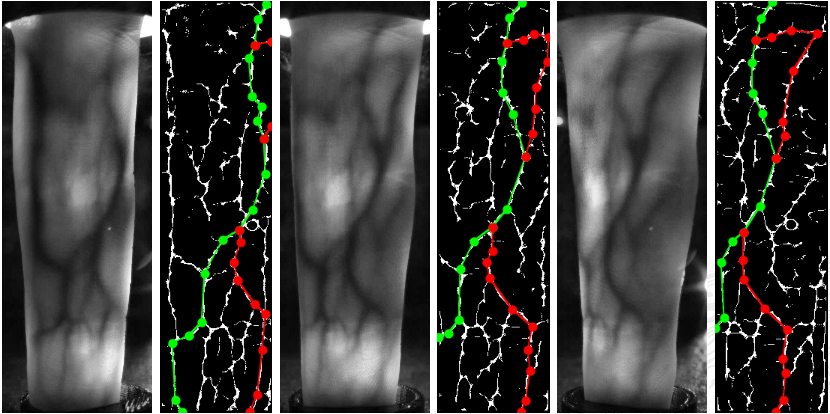

Figure: Examples of finger vein images and extracted MC features acquired at different longitudinal rotation angles. Left: -30°, middle: 0° (palmar view), right: 30°.

Outline

Experiments I

Systematic robustness analysis of several finger vein recognition schemes against longitudinal rotation.

- Palmar perspective = reference view
- Used range: $\pm 90°$, step size $1°$
- Cross-comparison of the rotated perspectives to the reference view
- Analysed the change of the recognition performance

Experiments II

Used recognition schemes:

- Vein pattern based feature extraction methods (binarization)
  - Maximum Curvature (MC) [4]
  - Principal Curvature (PC) [5]
  - Gabor Filter (GF) [6]
- Key-point based methods
  - SIFT [7]
  - Deformation-tolerant feature-point matching (DTFPM) [8]

Except for DTFPM, all methods are widely used and publicly available implementations exist.

DTFPM has been fully re-implemented and will be available at http://www.wavelab.at/sources/Prommegger18b/

Performance indicator:

- EER (FMR = FNMR)
- FMR1000 (the lowest FNMR for FMR = 0.1%)
- ZeroFMR (the lowest FNMR for FMR = 0%)
- Relative performance degradation (RPD):

$$RPD = \frac{EER_{current} - EER_{reference}}{EER_{reference}} \quad (1)$$

Baseline performance results (palmar view, 0°) for the different recognition schemes:

	PC	MC	DTFPM	SIFT	GF
EER [%]	**0.48**	0.59	1.15	1.53	3.14
FMR1000 [%]	0.79	0.83	2.54	4.88	5.40
ZeroFMR[%]	1.51	1.31	3.93	6.43	7.82

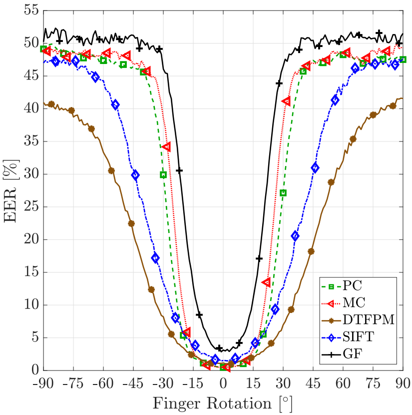

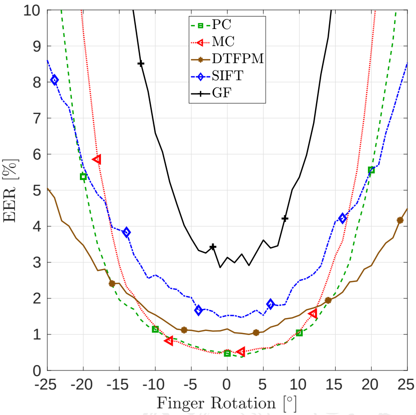

Figure: Trend of the EER across the different rotation angles, left: -90° to 90°, right: -25° to 25°.

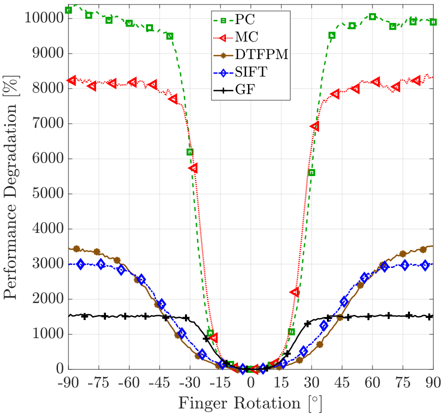

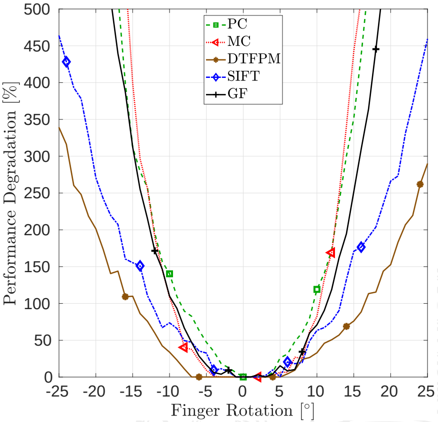

Figure: Trend of the relative performance degratation (RPD) across the different rotation angles, left: -90° to 90°, right: -25° to 25°.

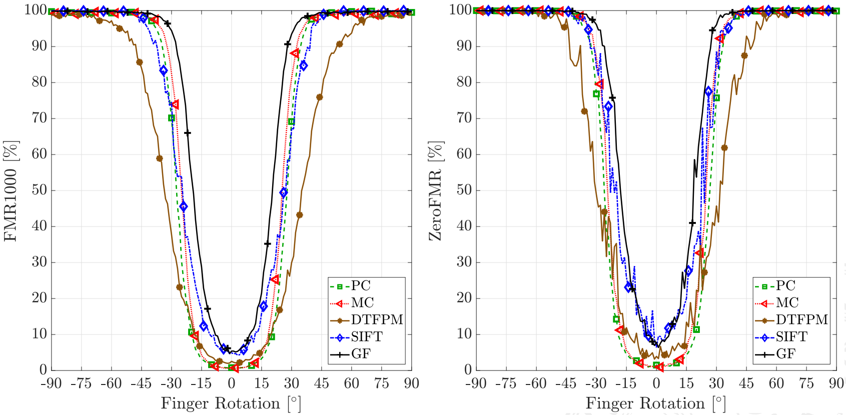

Figure: Trend of performance indicators across the different rotation angles from -90° to 90°, left: FMR1000, right: ZeroFMR in %.

Experiments VII

EER at specific rotation angles [%]:

	±0°	±5°	±10°	±15°	±20°	±25°	±30°	±45°
PC	**0.48**	**0.60**	**1.04**	**1.96**	5.38	13.43	27.14	46.50
MC	0.59	0.62	1.07	2.92	8.88	22.34	37.91	46.82
DTFPM	1.15	1.07	1.53	2.03	**2.91**	**4.49**	**6.97**	**19.26**
SIFT	1.53	1.53	2.49	3.90	5.59	8.53	12.61	30.15
GF	3.14	3.62	5.36	11.03	22.70	37.86	46.06	50.46

- Up to ±10° PC and MC perform best
- Starting with ±15° DTFPM outperforms all other schemes
- Starting with ±20° SIFT outperforms all vein pattern based schemes

Experiments VIII

Relative performance degradation at specific rotation angles [%]:

	$\pm 0°$	$\pm 5°$	$\pm 10°$	$\pm 15°$	$\pm 20°$	$\pm 25°$	$\pm 30°$	$\pm 45°$
PC	**0**%	26%	119%	312%	1031%	2727%	5610%	9684%
MC	**0**%	7%	83%	399%	1416%	3715%	6373%	7894%
DTFPM	**0**%	**0**%	**33**%	**76**%	**153**%	**290**%	**505**%	1573%
SIFT	**0**%	**0**%	63%	155%	266%	459%	726%	1876%
GF	**0**%	15%	71%	252%	624%	1107%	1369%	**1509**%

- DTFPM performs best (designed to be so)
- Values need to be read carefully (calculated to baseline result, baseline result different for every method)

Rotation angle at which a certain relative performance degradation is hit:

	10%	25%	50%	100%	200%	300%	400%	500%
PC	±1°	±3°	±5°	±8°	±12°	±13°	±15°	±16°
MC	±5°	±6°	±8°	±9°	±12°	±13°	±14°	±15°
DTFPM	±**7**°	±**8**°	±**11**°	±**14**°	±**19**°	±**23**°	±**26**°	±**28**°
SIFT	±4°	±4°	±8°	±12°	±16°	±20°	±23°	±25°
GF	±4°	±5°	±7°	±9°	±12°	±14°	±16°	±17°

- Key-point based methods perform better than vein pattern based methods
- All vein pattern based methods show the same trend

Outline

Conclusion and Future Work I

Contribution:

- Designed a custom rotating multi-perspective finger vein scanner device
- Established the first multi-perspective finger vein data set (360°-view)
  - Will be made available to the public in the future
- Systematic robustness analysis of several finger vein recognition schemes against longitudinal finger rotation
- Publicly abailable implementation of DTFPM

Conclusion and Future Work II

Conclusion

- Up to ±10° all schemes can handle longitudinal rotation.
- Key-point based algorithms (DTFPM, SIFT) are more tolerant against this kind of deformation.
- Above ±30° a reliable recognition is not possible at all.

An implementation of all recognition schemes, the scores and detailed results will be available at:

`http://wavelab.at/sources/Prommegger18b`

Conclusion and Future Work III

Future Work

- Verify to which extend longitudinal rotation can be corrected
  - by using the known rotation angle (PLUSVein-Finger Rotation Data Set)
  - by detecting/estimating the angle (e.g. like Chen et al. [9])
- Try to find new algorithms to reduce the effect of longitudinal finger rotation.

Thank you!

Q & A

Outline

Bibliography I

[1] B. Prommegger, C. Kauba, and A. Uhl, "Multi-perspective finger-vein biometrics," in *Proceedings of the IEEE 9th International Conference on Biometrics: Theory, Applications, and Systems (BTAS2018)*, Los Angeles, California, USA, 2018, pp. 1–9.

[2] University of Reading, "PROTECT Multimodal DB Dataset," June 2017, available by request at http://projectprotect.eu/dataset/.

[3] C. Kauba, B. Prommegger, and A. Uhl, "Focussing the beam - a new laser illumination based data set providing insights to finger-vein recognition," in *Proceedings of the IEEE 9th International Conference on Biometrics: Theory, Applications, and Systems (BTAS2018)*, Los Angeles, California, USA, 2018, pp. 1–9.

[4] N. Miura, A. Nagasaka, and T. Miyatake, “Extraction of finger-vein patterns using maximum curvature points in image profiles,” *IEICE transactions on information and systems*, vol. 90, no. 8, pp. 1185–1194, 2007.

[5] J. H. Choi, W. Song, T. Kim, S.-R. Lee, and H. C. Kim, “Finger vein extraction using gradient normalization and principal curvature,” *Proc.SPIE*, vol. 7251, pp. 7251 – 7251 – 9, 2009. [Online]. Available: https://doi.org/10.1117/12.810458

[6] A. Kumar and Y. Zhou, “Human identification using finger images,” *Image Processing, IEEE Transactions on*, vol. 21, no. 4, pp. 2228–2244, 2012.

Bibliography III

[7] C. Kauba, J. Reissig, and A. Uhl, "Pre-processing cascades and fusion in finger vein recognition," in *Proceedings of the International Conference of the Biometrics Special Interest Group (BIOSIG'14)*, Darmstadt, Germany, sep 2014.

[8] Y. Matsuda, N. Miura, A. Nagasaka, H. Kiyomizu, and T. Miyatake, "Finger-vein authentication based on deformation-tolerant feature-point matching," *Machine Vision and Applications*, vol. 27, no. 2, pp. 237–250, 2016.

[9] Q. Chen, L. Yang, G. Yang, and Y. Yin, "Geometric shape analysis based finger vein deformation detection and correction," *Neurocomputing*, 2018. [Online]. Available: https://www.sciencedirect.com/science/article/pii/S0925231218306192